TRANSFER REPORT

ON

Investigation of human chromosome aberrations using Fluorescence Lifetime Imaging Microscopy (FLIM)

Department of Chemistry
University College London, UK
May 21, 2018

Name: Miss Archana Bhartiya
Supervisor: Prof Ian Robinson
Placement Organisation: Research Complex at Harwell (RCaH), Oxford

DECLARATION

I, Archana Bhartiya confirm that the work presented in this thesis is my own. Where information has been derived from other sources, I confirm that this has been indicated in the report.

(London, May 2018)

LIST OF ABBREVATIONS

DNA	Deoxyribonucleic acid
CA/s	Chromosome aberration/s
G-bandings	Giemsa-bandings
FLIM	Fluorescence Lifetime Imaging Microscopy
AT	Adenine-Thymine
GC	Guanine- Cytosine
UV	Ultraviolet
LET	Linear Energy Transfer
DSB	Double strand breaks
NHEJ	Non-Homologous End Joining
HR	Homologous Recombination
Gy	Gray (unit of absorbed radiation dose by the cell)
FISH/mFISH	Fluorescence In suite Hybridisation/multiplex FISH
FRET-FLIM	Forster Resonance Energy Transfer-FLIM
s	Seconds
TCSPC	Time-Correlated Single Photon Counting
DAPI	4',6-diamidino-2-phenylindole
Vdw	Vander waal force
FBS	Fetal Bovine Serum
RPMI-160 (1x)	Roswell Park Memorial Institute
PHE	Public Health England
mins	Minutes
hrs	Hours
KCL	Potassium chloride
MAA	Methanol acetic acid
µl	Microliter
rpm	Revolutions per minute
CLF	Central Laser Facility
RCaH	Research Complex at Harwell
FLImP	Fluorophore Localisation Imaging with Photo-bleaching

LIST OF FIGURES

LIST OF TABLES

TABLE OF CONTENTS

1. PRINCIPLES OF RESEARCH

Radiation exposure causes mutations in deoxyribonucleic acid (DNA) leading to chromosome aberrations (CAs) and subsequent diseases such as cancer. The effect of radiation can also affect individuals but also offspring. This has been studied by investigating chromosomes after Hiroshima and Nagasaki atomic bomb attacks in World War II[1]. Karyotype analysis using conventional microscopy helps to understand the effects of radiation on chromosomes. In addition, karyotyping is also used in clinical applications before proceeding with medical treatments [2].

Genetic material is compact in the form of chromosomes to store information and protect genomic DNA from internal and external damage. The heterochromatin regions present in a chromosome prevent genetic information from aberrations and helps in gene regulation. The centromeres, large structures where the two chromosome arms are attached together, are necessary for proper segregation of chromosomes. Though, the compaction of DNA into chromosomes is important; still it is not fully understood how DNA is packed into chromosomes.

This report investigates the effect of X-ray radiation on the structure of human chromosomes. Then the frequency of chromosomal aberration transferred from one cell cycle to another is also studied. Accordingly, cells are X-ray irradiated to see the effects of radiation on human chromosomes using Fluorescence Lifetime Imaging Microscopy (FLIM) [3] technique.

To measure the life time changes in X-ray induced chromosomes the FLIM technique was employed. FLIM is a time and frequency domain [3,4] dependent, microscopy technique which measures the lifetime of fluorophores depending upon the environment of the molecules. It is hypothesised that FLIM can make it possible to understand the effect of irradiation on the structure of human chromosomes.

Work to date indicates that FLIM has been used to identify compact heterochromatic regions (proximity to centromere) in undamaged metaphase chromosomes [5]. FLIM has also been used to study condensation of chromosomes with regulation of divalent ions [6].

My future work will focus on investigating on how does the X-ray radiation effects the compaction of fixed metaphase human chromosomes at different radiation dose and whether it will be detected by FLIM technique ?

2. INTRODUCTION

2.1 Chromosome structure

Chromatin are DNA-protein complexes present in nucleated cells. They form a thread-like structure during interphase and slowly get condensed at the metaphase stage during cell division. DNA acquires different levels of packaging to fit within the approximately 10 μm nucleus of the cell fig 1. A 2 meter long DNA is wrapped around octamer histone proteins (H2A, H2B, H3 and H4) to form 11 nm nucleosomes referred to as "beads on a string" [7]. Histone H1 proteins are DNA linkers that form complex structures by linking nucleosomes together to maintain chromatin stability [8]. Nucleosomes are the building blocks of chromosomes. They supercoil to form a high-order structure known as the 30 nm chromatin fibre that then folds into a compact mitotic chromosome [9,10]. The 30nm structure has been reported as either Solenoid or Zigzag, [10] based on their unique coiling patterns. Other factors such as monovalent and divalent cations play important roles in regulating the high-order structures of chromosomes. The concentration of monovalent Na^+/K^+ and divalent Ca^{2+} /Mg^{2+} increases from interphase to metaphase in the cell cycle [8]. Human have 22 pairs of autosomes and one pair of sex chromosomes [11].

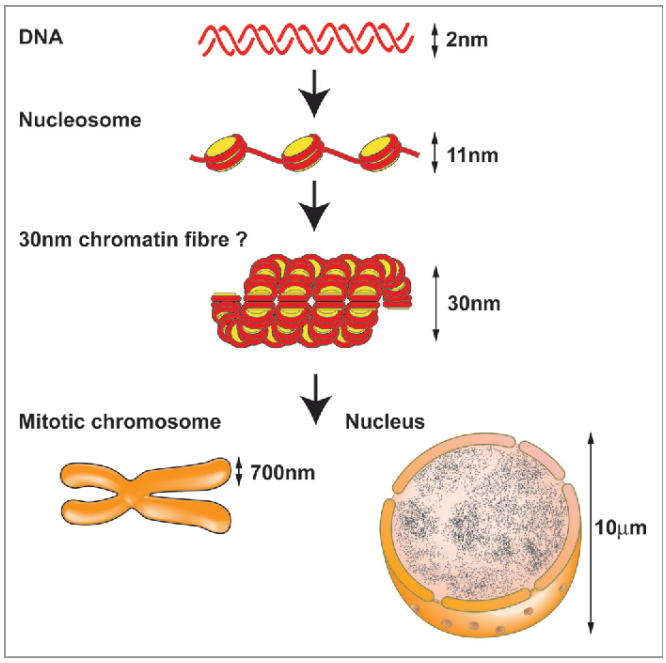

Figure 1: Packaging of human genome [10].

2.2 Karyotyping

A karyotype is a way of classifying the full genetic complement, when chromosomes are arranged according to their size and shape (fig 2). This is the first stage of identifying any genetic aberrations, like structural and numerical aberrations in an organism. Typically, chromosomes at the metaphase or prometaphase stage of the cell cycle are arrested and stained with an appropriate dye for karyotyping. Karyotyping has efficient clinical applications and can be used for diagnosing genetic diseases [2]. Several differential staining techniques are used to introduce visible "bands" in the structures. In G-bandings (Giemsa-bandings), the most commonly used staining protocol, the bands replicate during cell cycle and it can be either positive (dark) or negative (light) depending upon the dye used on different chromosomes [12]. The G-banding highlights dark colour at the AT regions (heterochromatin) and the light colour at the GC regions (Euchromatin) of a DNA [13]. The euchromatin in less densely packed whereas the heterochromatin is more tightly packed.

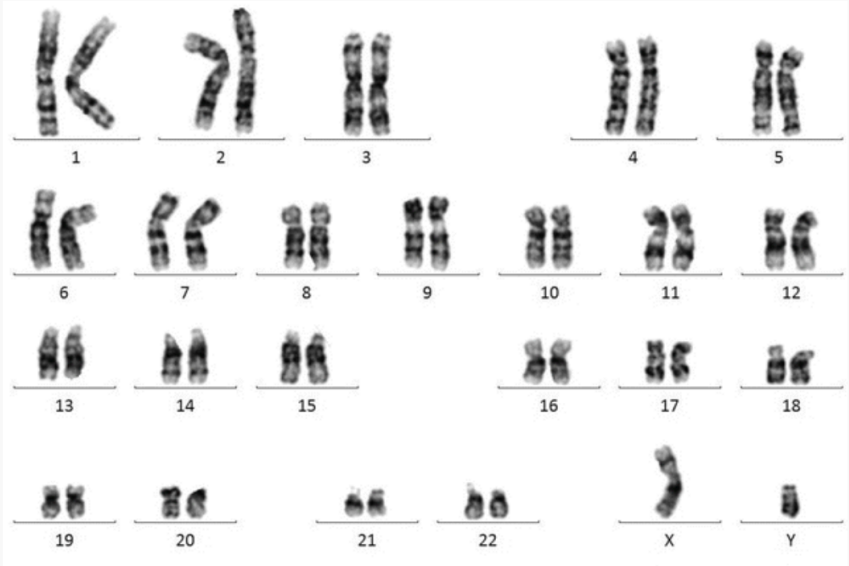

Figure 2: Karyogram of male human G-bands [14]

2.3 Human chromosomal aberrations

The gain, loss or translocation (switching strands) of genetic material within a chromosome is known as CAs (fig 4). Aberrations can be caused by external factors like Ultraviolet (UV), exposures to sunlight, ionising radiation (X-rays, gamma rays) and toxic chemicals. On other hand, internal factors like unequal cell divisions, replication errors and the enzymatic reactions can also cause aberrations [15]. Exposure to radiation can cause simple or clustered DNA damage.

However, one or two aberrations per DNA helical turn leads to double DNA strand breaks [16]. The X-ray irradiation deposits some energy, characterised as low or high "Linear energy transfer" (LET) when passed through the biomolecules that results in chemical modifications in a DNA [16,17]. The energy absorbed by water content present in a biomolecule, causes water radiolysis, that breaks down water molecules into free radicals of H^+ and OH^- [18]. Furthermore, the free radicals form reactive recombination such as toxic superoxide that leads to DNA damage [19]. A recent finding confirms that apart from irradiated cells, the nearby, non-irradiated cells also become affected. This phenomenon is called the "Bystander effect" and it only occurs at low radiation dose [17]. Double strand breaks (DSB) inhibit the replication and the transcription process [20] in any upcoming cell divisions. All these CAs may cause major phenotypic problems; including cell death, mutations and genomic instabilities [21].

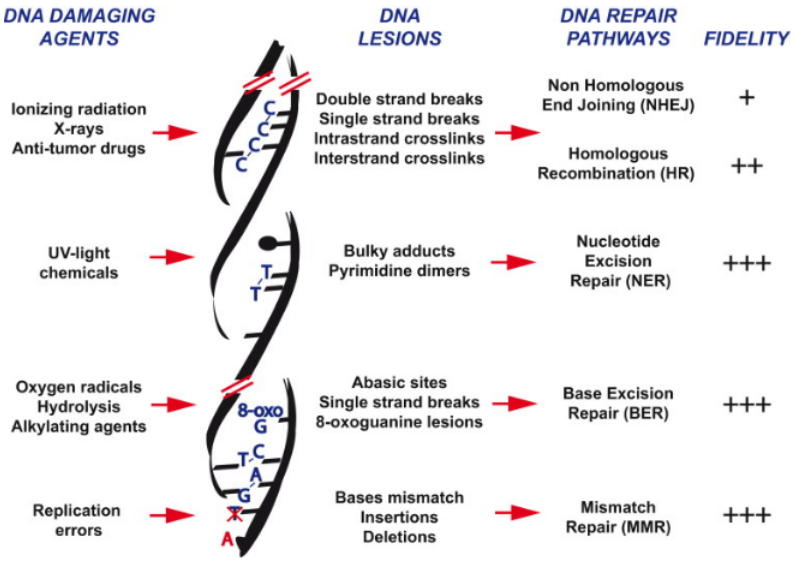

Figure 3: Potential regions prone to DNA damage and the response repair mechanism in mammalian cells [22].

There are two major types of chromosomal aberrations such as numerical and structural aberrations. Numerical aberrations consists of aneuploidy (occuring due to improper distribution of chromosomes at the anaphase stage of the cell cycle eg: trisomy and monosomy) and triploidy (missing of one homologous pair) [23]. These defects are known as non-dysjunction, and take place at mitosis and later at meiosis phase of the cell division [23]. The structural aberrations occur either due to breakage or irregular reunion, which is consequence of exposure to mutagens and/or ionising radiations.

The structural aberrations are classified as: i) duplication (gain of extra segment from another chromosomes), ii) deletion (loss of part of a chromosome), iii) translocation (transfer of DNA contents between homologues or non-homologous chromosome pairs), iv) inversion (rotation of gene sequence by 180 degrees), v) Isochromosomes (deletion of one arm with an addition of other), vi) dicentrics (presence of two centromeres in a chromosome) and vii) ring chromosomes (joining of two broken ends together) [23,24] (fig 4). Though, chromosome aberrations induce "sticky" breakpoint ends which become joined by repair mechanism such as Non-Homologous End Joining (NHEJ) and Homologous Recombination (HR) [22], with the help of specific enzymes (fig 3). Subsequently, failure of the repair process can produce large-scale rearrangements and recombination of the human genome and eventually causes disease such as cancer [25].

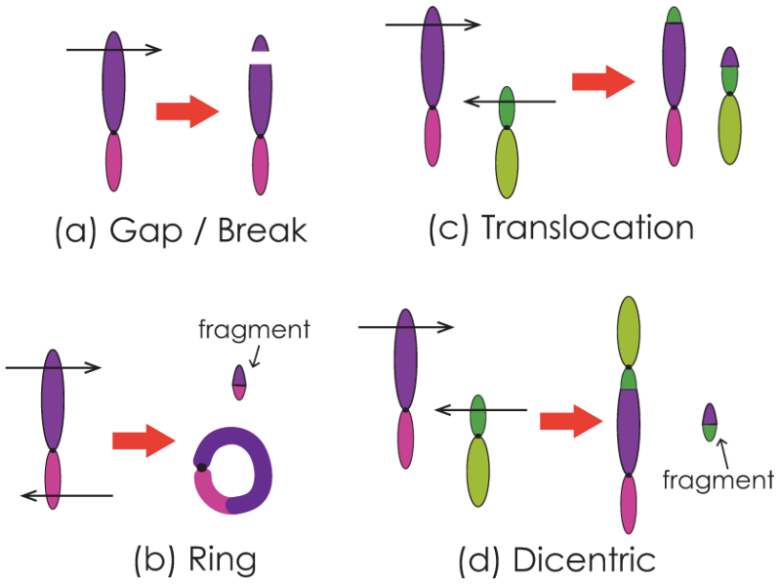

Figure 4: The four typical X-ray induced structural chromosomal aberrations [24].

When chromosomes are radiated with X-ray ionising radiation, mutations and unusual genomic behaviours occur. Cells irradiated with 1 Gray (1Gy = 100 rad, (unit of absorbed radiation dose by the cell)) to 2Gy can resist the radiation dose but slow down their cell division and their DNA damage repair mechanisms. Subsequently, they have a decrease in cell viability and can have acute levels of DNA damage, like exchanges and deletion of segments of chromosomes, though, this does not affect the transcription process [26]. Major aberrations usually occur with higher radiation doses starting from 1Gy to 5Gy. This leads to a decrease of metaphase chromosome numbers and an increase in the frequencies of dicentric, acentric

(with no centromere) and ring chromosomes [27]. Furthermore, the dicentric chromosome numbers decrease from first, to second, to third mitotic cell division. However, the number of acentric and the centric aberrations, which occurred due to deletion of telomeres, are found to increase from one mitotic cell division to another [28]. However, acentrics and the centrics could be the reason for CA transmission from subsequent mitotic cell cycles rather than dicentrics, and these leads to genomic instability.

Techniques used for CA analyses are Giemsa staining[12], Fluorescence *In Suite* Hybridisation (FISH) [29], flow cytometry and 24-colour multiplex Fluorescence *In Suite* Hybridisation (mFISH) [30]. These techniques have their limitations such as Giemsa metaphases can mislead the results, FISH and mFISH are insufficient to identify minor changes within chromosomes [31]. Flow cytometry is only significant for detecting numerical aberrations [32].

FLIM been valuable for the observations of chromosomal structural changes such as compaction of DAPI-stained fixed methanol acetic acid metaphase human chromosomes [5]. According to Estandarte *et al*, 2016, FLIM with undamaged fixed human metaphase chromosomes, show shorter lifetime in chromosome 1, 9, 15, 16 and Y at heterochromatic region compared to other chromosomes [5]. FLIM also has been used to see chromatin condensation in human endothelial cell nuclei at different viscosity environment [33]. Though, a shorter lifetime was observed in a condensed chromosome than in a de-condensed one. FLIM has ability to distinguish the affected and the unaffected cells caused by diseases. Chromosomes extracted from leukaemia affected cells showed shorter lifetime compared to the unaffected ones [34].

One of the important mechanisms underlying FLIM is the Forster Resonance Energy Transfer (FRET), which is also used to study protein-protein interactions and conformational changes in life science [4]. However, it is also employed to measure the compaction levels of a chromatin from interphase to telophase of the cell division. Interestingly, the FRET-FLIM combination can be used to understand the condensation and the de-condensation process of chromosomes, starting from prophase to prometaphase stage, happened due to regulation of concentration of calcium (Ca^{+2}) divalent cations in the cells [6].

2.4 Principle of FLIM

Fluorescence is a phenomenon that occurs when external photons excite the electrons of a molecule at the ground state level, the electrons after absorbing the light emit photons and the electrons come back to ground state with loss of energy. It is summarised in the Jablonski diagram of fig 5.

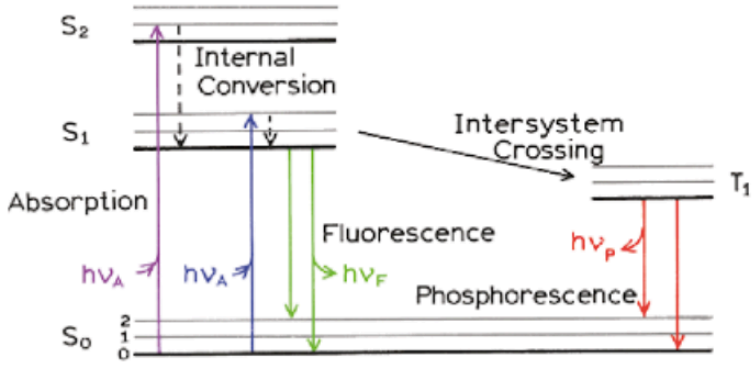

Figure 5: Jablonski diagram representing electronic energy levels [35].

The relaxation time correlates with the speed of internal molecular processes excited with incoming light. Absorbance typically lasts for approximately 10^{-15} seconds (s) while fluorescence lasts for 10^{-9} s [35,36]. The time during which the molecules stay in their excited state is called lifetime of fluorophore and it ranges from 10^{-8}-10^{-9} s [35].

Since each dye has its own lifetime in the excited state, FLIM can distinguish between unknown labelled dyes, by measuring lifetime change of each dye. The concept of FLIM is its ability to distinguish two regions of an image having same brightness but different lifetime whereas an intensity image is unsuccessful to differentiate the same [37]. Hence, the FLIM image gives more information than the intensity image.

FLIM is neither affected by photo-bleaching nor auto-fluorescence (which affect only the intensity) and has potential for single molecule monitoring [3]. Photo-bleaching and the signal to noise ratio can be reduced unlike other fluorescence microscopy methods by adjusting the scan time of the samples and altering laser power according to the requirements to gain good resolution [38]. The main advantage of FLIM is that it is independent of the concentration of

fluorophores. It calculates the lifetime from environmental change in the sample such as pH, viscosity, temperature, refractive index, ion concentrations and quantum efficiency of the probes [4].

To acquire FLIM data, samples are raster scanned in X and Y coordinates under high power Ti-sapphire laser pulses. The emitted photons are counted by Time-Correlated Single Photon Counting (TCSPC) within each individual pixel with respect to time. Integrated photons are sent to SPCImage software, to fit exponential decays at each pixel into get the lifetime of decayed fluorophores within each element [38].

2.5 DNA-DAPI binding dye

Molecular probes with higher quantum yield and longer lifetime give better contrast images. 4',6-diamidino-2-phenylindole (DAPI) is a popular nucleic acid stain, binding to AT-rich regions of DNA every 2-3 base pairs. It absorbs light at 350nm wavelength and emits blue fluorescence at 470nm wavelength. It works with 405nm lasers. The quantum yield of DAPI is 0.92. When DAPI bounds to DNA it greatly improves contrast of an image because the quantum yield is much smaller for unbound dye in solution.

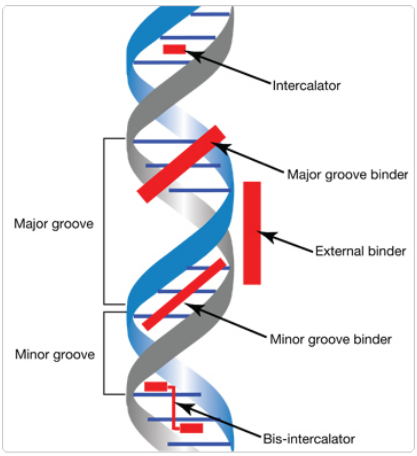

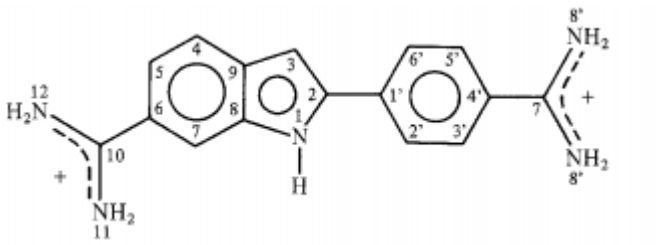

Figure 1 (a): Chemical structure of 4',6-diamidino-2-phenylindole (DAPI) [39].

Figure 6 (b): Double strand DNA with bound dyes [40]

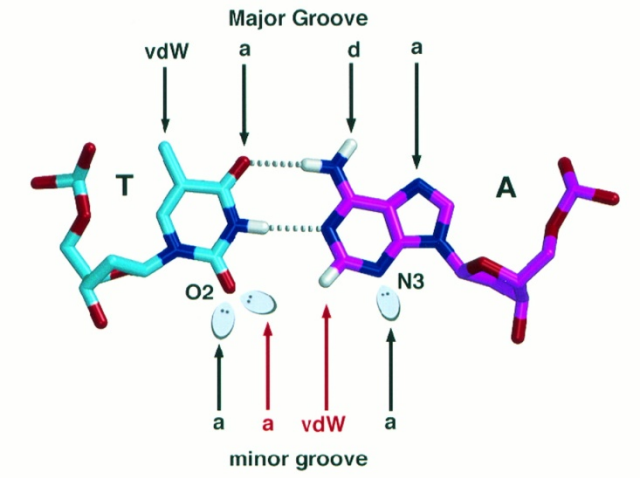

Figure 6 (c) : Minor groove of a DNA demonstrates DAPI binding regions [41].

The fig 6a shows the molecular structure of a DAPI with three hydrogen donor group, 2 amidino moieties at the end and one NH indole group carrying a positive charge that strongly interact with the three hydrogen-bond acceptor(a) regions of DNA (N3 of adenine and O2 of thymidine) in the minor grooves of the AT-rich regions. Hydrogen bonding and van der Waals (Vdw) forces as shown in fig 6c which form the DNA-DAPI complex [41].

The fluorescence lifetime of a DNA-DAPI complex depends on various factors such as i) the specificity of a DAPI to bind AT-rich regions of DNA at minor grooves ii) DAPI is more prone to AT base pairs than GC because of presence of amino acid at the position 2 of an adenine iii) the complex has low anisotropy because of highly coiled structure of DNA. iv) The proton transfer process is inhibited when DAPI binds to AT clusters than GC clusters which increases its lifetime. These properties of DAPI makes it more specific to bind DNA and helps in structural determination of DNA and DNA- chromosomes. The spectroscopy lifetime varies substantially on binding: the DNA-DAPI complex has 2.8ns bound with AT and 0.2ns for unbound DAPI in solution [39].

3. MATERIALS AND METHODS

3.1 Cell culture and cell count

The media is prepared by mixing, 20% of fetal bovine serum (FBS), 1% of penicillin (100U/ml), 1% of streptomycin (100µg/ml), and 1% of L-Glutamine (2mM) into a Roswell Park Memorial Institute (RPMI-1640 (1X), Sigma Aldrich, UK) medium. The prepared medium is incubated at 37°C water bath before use. Suspension human B-Lymphocyte (GM18507, International HapMap Project, Yoruba male) were used. The cells were taken out from the liquid nitrogen, thawed and cells were (1mL) transferred to T25 cell culture flask under Laminar Air Flow (LAF). Immediately incubated at 37°C with 5% supply of CO_2 for 3-4 days to get good growth of cells. After 3 days, cells were transferred from a T25 to T75 flask and allowed growing for subsequent splitting. The density of the cells was obtained by performing cell count. Mixing 10 microliter (µl) of the sample plus 10µl of Trypan blue dye (0.4%, Life Technology) in an eppendrof. 10µl of the mixture was pipette onto the cell counting slide (BIO-RAD), and a measurement was taken.

3.2 X-ray irradiated cells

The confluent cells, up to 85% , were transferred to T25 cell culture flask, 5ml in each flask. Cells were taken to X-ray facility, Public Health England (PHE) for irradiation. Flask containing 5ml of cell media were irradiated with hard X-ray doses of 0.1Gy, 0.2Gy, 0.5Gy, 1Gy and 2Gy with duration of 12s , 24s, 1 minutes (mins), 2mins and 4mins respectively. The energy of X-ray was 250KVp at dose rate of 0.5Gy/min. After irradiation, the cells were transferred into falcon tube and spun for 1200rpm for 10mins, supernatant discarded, fresh 5ml RPMI-1640 media were added and incubated at 37°C. Five flasks were kept for 24 hours (hrs) and five for 48hrs, aimed to attain first and second phase of the human cell cycle.

3.3 Chromosome preparation

After 24hrs and the 48hrs of incubation at 37°C with 5% supply of CO_2, 0.2µgml^{-1} of colcemid (Karyomax, Gibco by Life technologies (10µgml^{-1}) was added to 5 ml of media to arrest the cells at prophase/metaphase. After 6 hours of colcemid treatment; the media was discarded into

virkon solution and 37°C pre-warmed 6ml hypotonic potassium chloride solution (75mM KCL) was added slowly. Following this step, cells were incubated at 37°C water bath for 8-10mins and then spun at 1200 revolution per minute (rpm) for 5mins. Discarded supernatant and added freshly prepared 6ml fixative, methanol: acetic acid (MAA,3:1) and spun at 1200rpm for 5mins. Discarded supernatant and repeated two washes of MAA to get crystal clear solutions and finally stored in the freezer for future use.

3.4 Chromosome mounting

The glass slides (Supersoft) were cleaned by soaking overnight in 70% ethanol, effectively removes grease, wiped slides with soft tissues and placed in the freezer for 30mins. While chromosomes spread (46 chromosomes) preparation, took out the slides from the freezer, blew on the slides to make it humid and dropped 20 µl -30 µl of MAA fixed chromosomes sample from a height to obtain sufficient numbers of good spreads of chromosomes. Prepared slides were kept on the hot plate (40°C) to dry for 5mins – 10mins, stained with 4µM DAPI (ThermoFisher Scientific) and incubated for 15mins, away from light. Stained slides were soaked in a PBS (pH-7.4(1X), Phosphate Buffered Saline) for 4 mins to get rid of unbound DAPI, rinsed with water, mounted with water and placed cover slip (22 x 50, No.1.5) on the slides and taken for imaging. Prepared slides were first observed under fluorescence microscope (Zeiss Z2 Axio imager with Isis software) to check maximum number of good spreads on the prepared slides. Finally, slides were taken for FLIM imaging.

3.5 FLIM microscope setup

A multiphoton excitation microscopy technique was used to acquire the lifetime of methanol acetic acid (3:1, MAA) fixed metaphase human chromosome spreads, cells were X-ray irradiated at PHE. The multiphoton microscope is located at the Central Laser Facility (CLF) in the Research Complex at Harwell (RCaH), UK. Brief description of the set-up as follow; the sample was placed onto a stage of Nikon Eclipse confocal microscope to scan and to locate the sample with 405nm blue laser, the laser excites DAPI and produce fluorescent image of the chromosome spreads. Then 405nm laser turned off and the multiphoton Ti-Sapphire laser is switched on, to raster-scanned the sample with the Ti-sapphire laser through x60, NA 1.2 water immersion objective at laser power of 80MHz and the detector used (HPM-100-50) to detect the photons. Then, TCSPC, FLIM module (SPCM-830) from Becker & Hickl was used to

record the arrival time of the photons while scanning each x and y coordinates, and the data sent to SPCImage software for data analysis and measure fluorescence lifetime of each chromosomes.

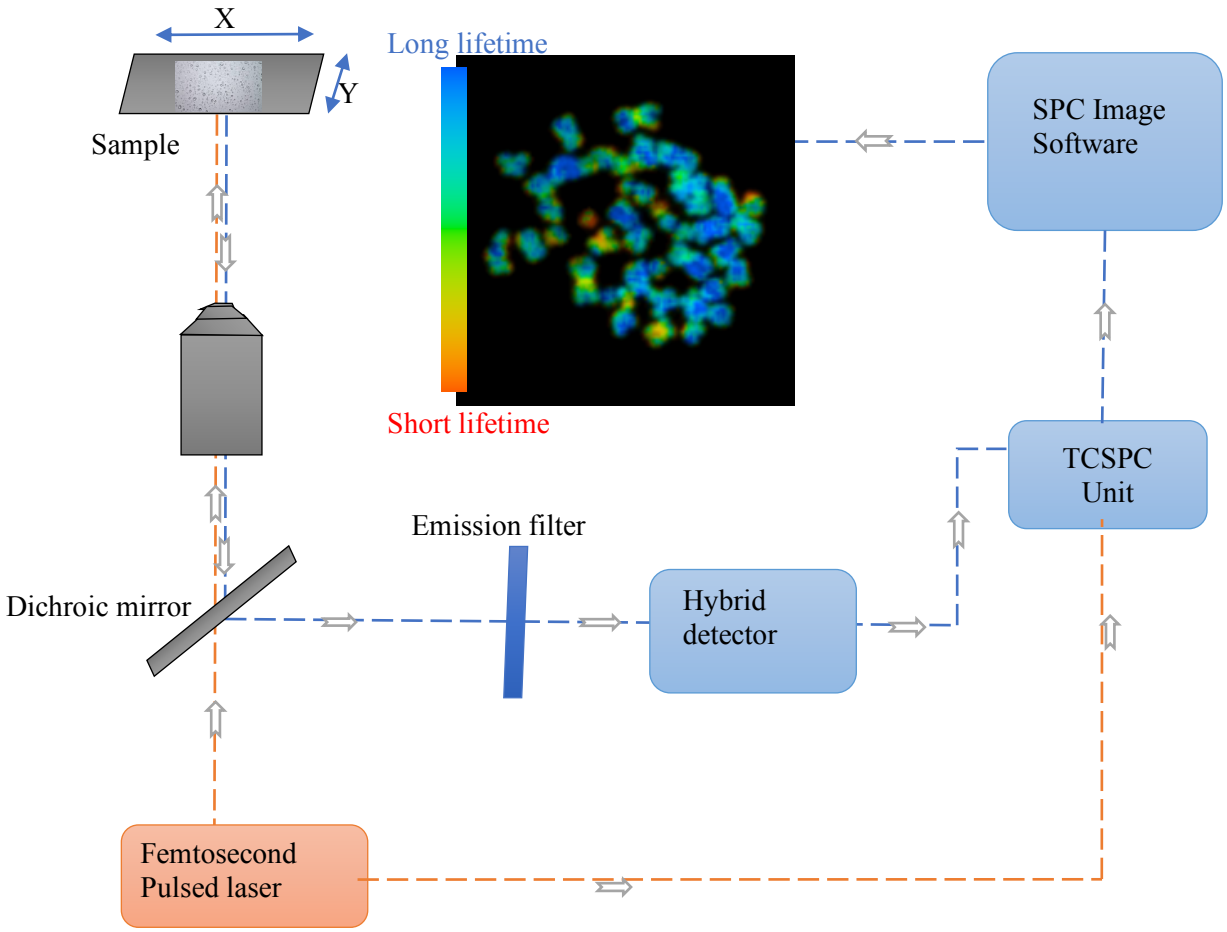

Figure 7: Schematic of a FLIM setup for chromosome imaging.

3.6 Analysis of a FLIM data

Chromosome samples are laser scanned at X and Y coordinates with period of laser pulses, number of arrived photons counted by TCSPC at time "t" and at each pixel. Then data is sent to SPCImage software (Becker and Hickl) to fit obtained exponential decays from each pixel to get lifetime of decayed fluorophores by fitting the decay curves into a multi-exponential algorithms [38]. We used "incomplete multi-exponential decay" [42] model and the χ^2 value should be close to unity for perfect decay fit [43], to measure accurate fluorescence lifetime of a fluorophore. Then pseudo coloured histogram is generated which denotes lifetime change obtained at the pixel-level to produce an image. FLIM delivers information about the spatial

distribution of a fluorescent molecule together with information about their nano-environments. Henceforth, in fig 7, the chromosome spread, regions coded with blue colour correspond to a long lifetime change and the regions coded red colour correspond to a short lifetime change.

4. PRELAMINARY RESULTS

4.1 Fluorescence of DAPI bound to damaged fixed metaphase chromosomes

The aim is to understand two causes of lifetime changes: i) the effect of X-ray ionising radiation in chromosomes aberrations and ii) the effect of compaction of chromosomes with ions. Methanol acetic acid fixed human metaphase chromosome samples are used throughout as a standard. The structure/morphology of a chromosome is considered the major determinant of chromosome aberrations. In this project, we are investigating the compaction and the variant structural chromosomal aberrations, transmitted from one cell cycle event to another, starting from the first mitosis after irradiation.

Human B-lymphocyte cells were X-ray irradiated at dose rate of 0.5Gy/min at 250KVp energy. Chosen doses for irradiation were 0.1Gy, 0.2Gy, 0.5Gy, 1Gy, 2Gy, 5Gy and 10Gy. Then the cells were left to divide at different intervals such as 24hrs, 26hrs, 48hrs and 50hrs. Metaphase chromosomes were extracted from irradiated cells and fixed with methanol acetic acid (3:1). Later samples were dropped from a height onto the glass slide to obtain many metaphase chromosomes spreads (46-chromosomes) and stained with DAPI to analysis under fluorescence microscopy. Metaphase spreads were located under the Zeiss cytogenetic microscope, to find those with visible aberrations. The coordinates were recorded and then taken for lifetime measurements on the FLIM system.

4.1.1 Aberrations after 24hrs of irradiation

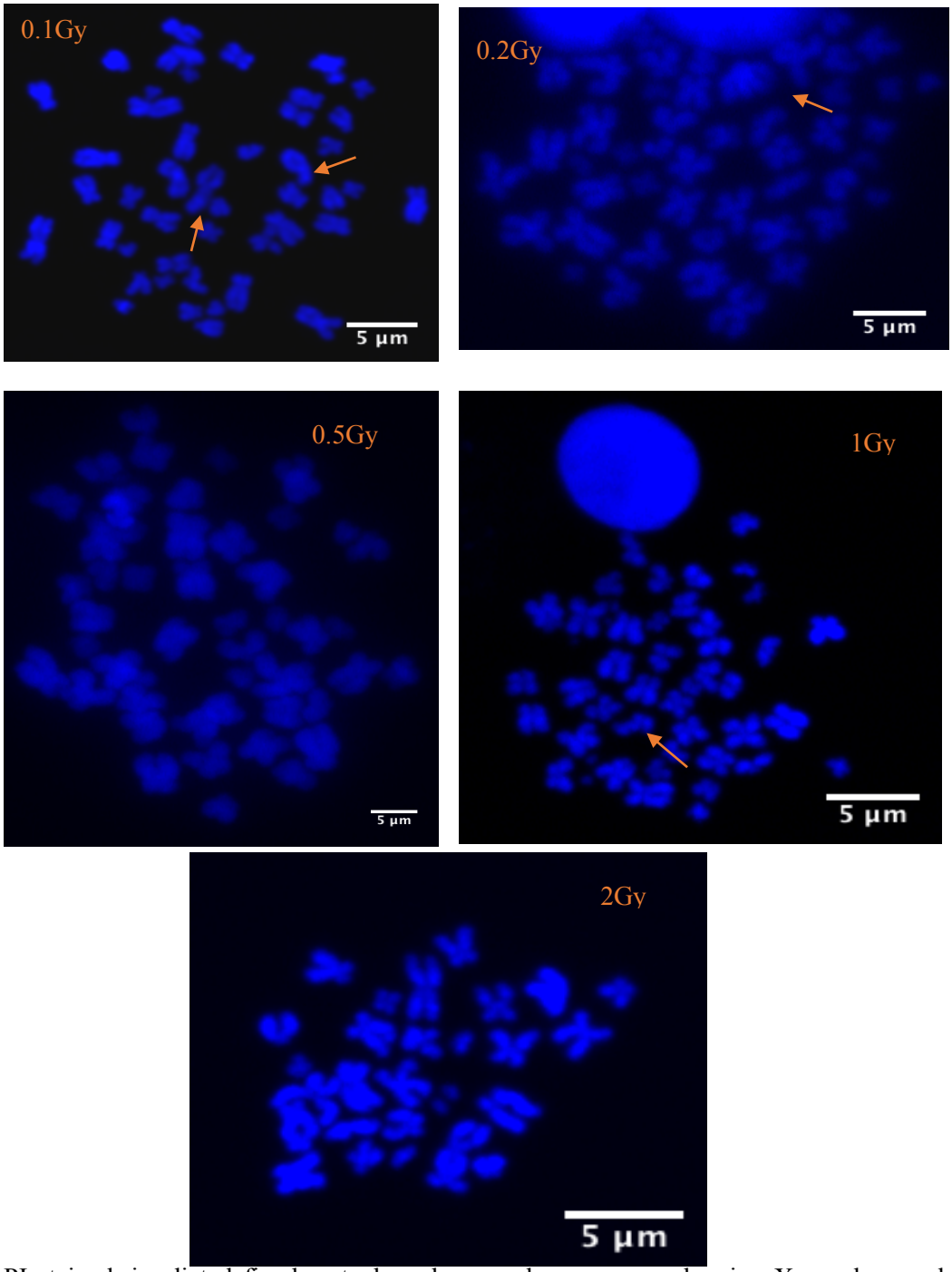

Figure 8: DAPI stained, irradiated fixed metaphase human chromosomes showing X-ray dose and number of survived chromosomes after 24hrs of irradiation. At dose of 0.1Gy(46-chromosomes), 0.2Gy(46-chromosomes), 0.5Gy(46-chromosomes), 1Gy(46-chromosomes) and 2Gy(30-chromosomes). Arrows show one fused arm in 0.1Gy, joining of centromere of two chromosomes in 0.2Gy, missing of chromatid arm in 1Gy. 63x oil immersion objective images, scale bar-5µm.

We used ImageJ software to count the number of the chromosome present in each spread. After 24hrs of irradiation, normal chromosome numbers were maintained from 0.1Gy to 1Gy, but at 2Gy chromosomes the number decreases to 30, irrespective of normal counting. Major aberrations seen in 24hrs of irradiation were fused (fig 8, 0.1Gy) and "smashed" (Fig 8, 1Gy) arms of chromosomes.

4.1.2 Aberrations after 26hrs of irradiation

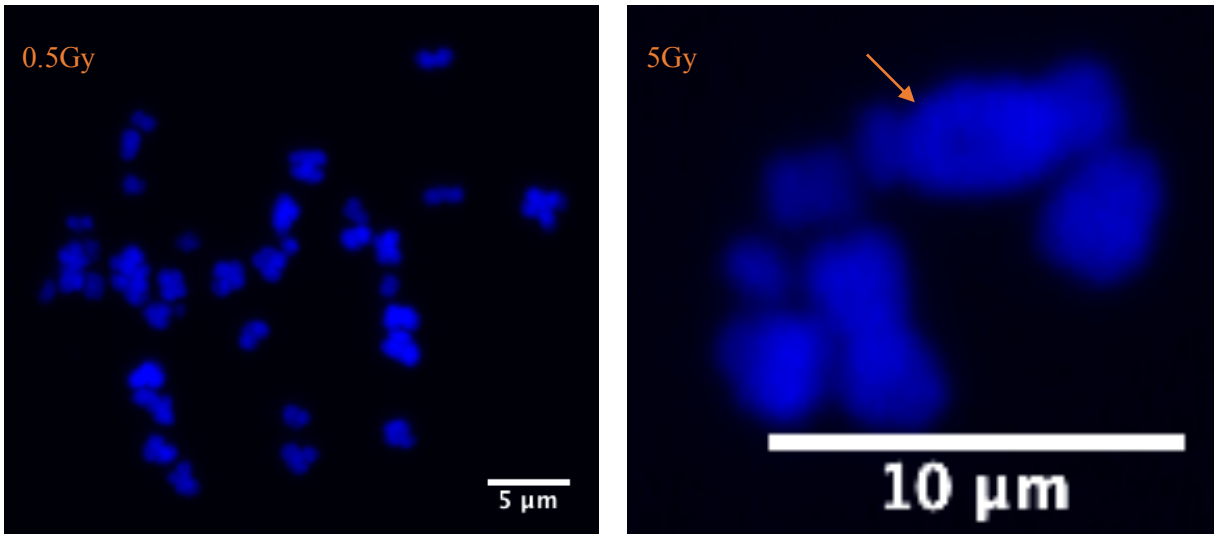

Figure 9: DAPI stained, irradiated fixed metaphase human chromosomes showing X-ray dose and number of survived chromosomes after 26hrs of irradiation. After doses of 0.5Gy (40-chromosomes, Scale bar-5µm) and 5Gy (6-chromosomes). Arrows show dicentric chromosomes following 5Gy X-ray dose, scale bar-10µm. 63x oil immersion objective images.

Even with after 26hrs of irradiation, dicentric chromosomes (fig 9, 5Gy) were observed and not enough metaphase chromosomes spreads were seen which makes us think that not enough cells/nuclei underwent normal cell division, probably because of a cell death or disruptions to a normal cell cycle due to an irradiation. After observation of 3-4 metaphase spreads it is concluded that at higher dose, starting from 5Gy, not enough cells undertake cell division due to cell death or double DNA strand breaks. In 5Gy (fig 9), scale bar is 10µm because of joining of two chromosomes to form a dicentric.

4.1.3 Aberrations after 48hrs of irradiation

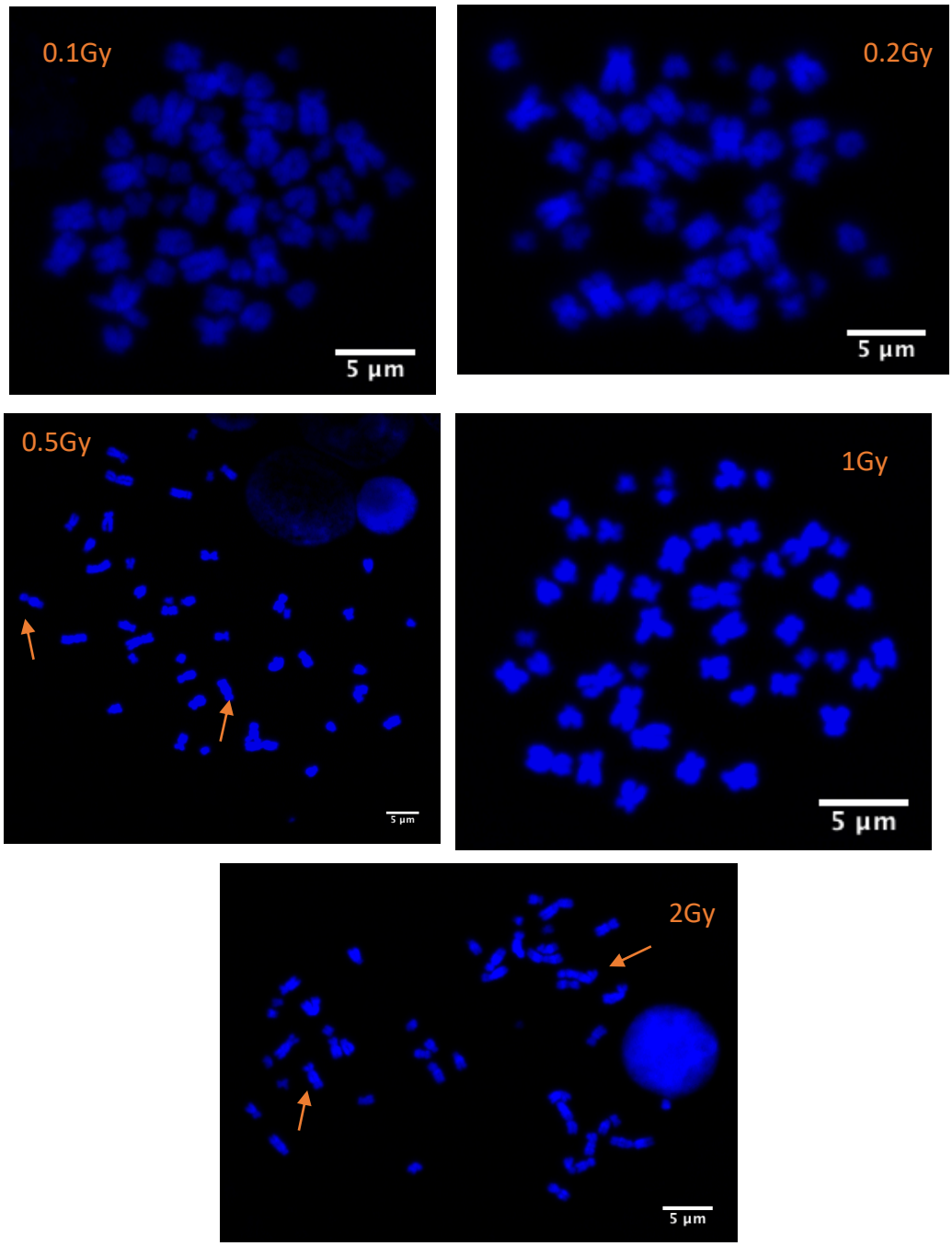

Figure 10: DAPI stained, irradiated fixed metaphase human chromosomes showing X-ray dose and number of survived chromosomes after 48hrs of irradiation. At doses of 0.1Gy(46-chromosomes), 0.2Gy(46-chromosomes), 0.5Gy(46-chromosomes), 1Gy(46-chromosomes) and 2Gy(46-chromosomes). Arrows show presence of dicentric and possibility of fragments of chromosomes in 2Gy. 63x oil immersion objective images, scale bar-5µm.

After 48hrs of irradiation, dicentrics were observed in 0.5Gy and 2Gy and possibility of presence of chromosome fragments in 2Gy (fig 10) of irradiation. More numbers of dicentric chromosomes were observed in second mitotic cycle (48hrs) compared to the first mitotic cycle (24hrs).

4.1.4 Aberrations after 50hrs of irradiation

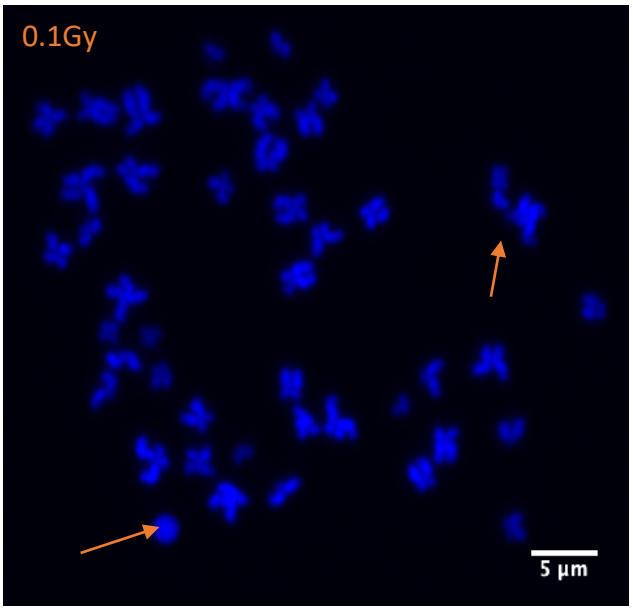

Figure 11: DAPI stained, irradiated fixed metaphase human chromosomes showing X-ray dose and number of survived chromosomes after 50hrs of irradiation. At doses like, 0.1Gy(46-chromosomes). Arrows show ring chromosomes, fragmented and damaged chromatid arms. 63x oil immersion objective images, scale bar-5µm.

In 50hrs of irradiation; following aberrations were observed like a ring chromosome, damaged chromatid arms and fragmented chromosomes.

4.2 FLIM of DAPI bound to non-X-ray irradiated fixed metaphase chromosomes

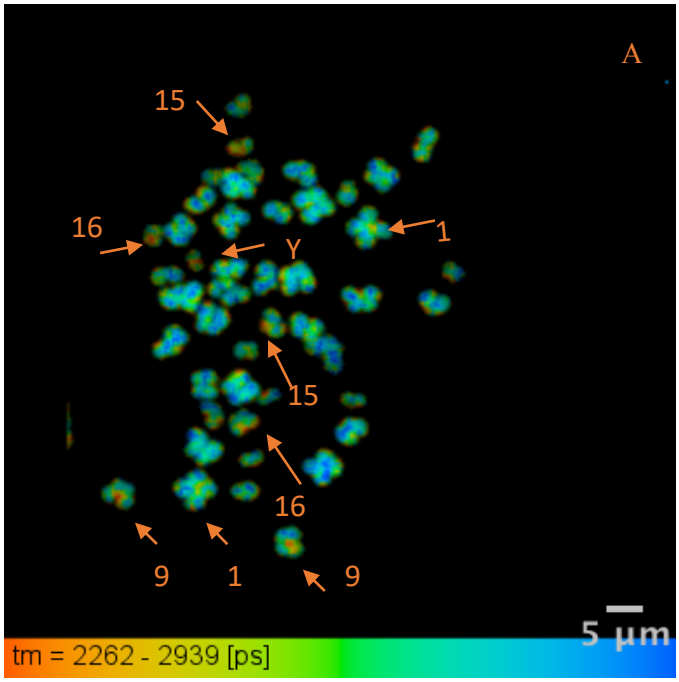

Chromosomes B	Mean lifetime ± SD, (ns)
1	2.66 ±0.04
9	2.55 ±0.07
15	2.44 ±0.03
16	2.46 ±0.01
Y	2.42

Figure 12: A) FLIM image of a non-X-ray irradiated fixed human metaphase chromosomes stained with 4µM DAPI and imaged with 60x water objective. B) Measured average lifetime of each heterochromatic chromosomes of image A. Standard Deviation (SD) represents varied lifetime in heterochromatic regions.

4.3 FLIM of DAPI bound to irradiated fixed metaphase chromosomes

For FLIM analysis, irradiated fixed metaphase spreads were prepared on the glass slides, stained with 4µM freshly prepared DAPI and then taken for fluorescence lifetime measurement using multiphoton microscopy. Metaphase spreads were extracted after 24hrs and the 48hrs of mitotic cell cycle, after X-ray irradiation and imaged under 60x water objective.

4.3.1 Aberrations after 24hrs of irradiation at 0.1Gy

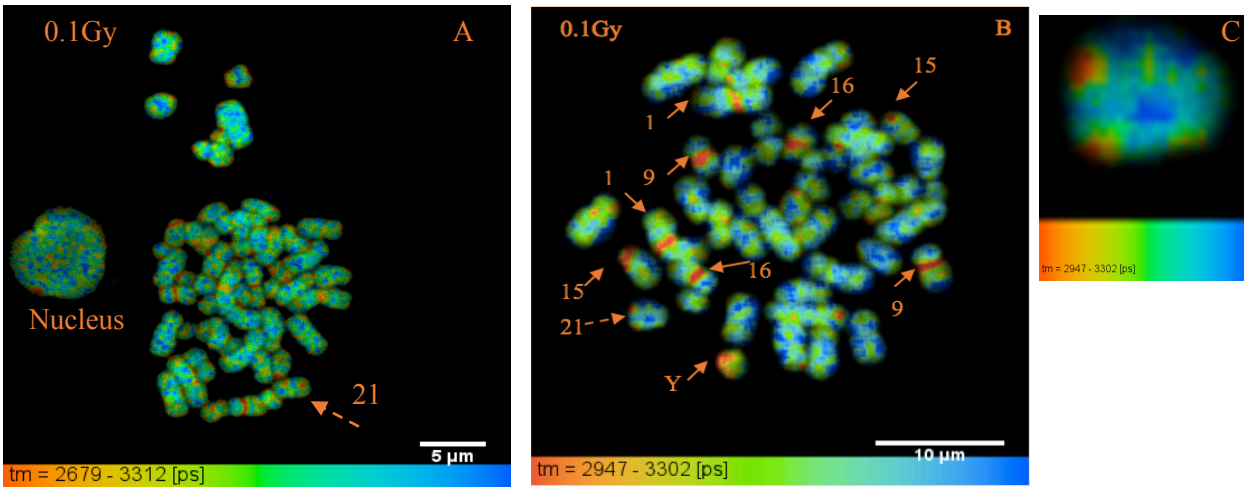

Figure 13: FLIM image of irradiated fixed human metaphase chromosomes stained with 4µM DAPI and imaged with 60x water objective. Two different spreads of metaphase chromosomes extracted after 24 hours of irradiation at 0.1Gy dose. Pseudo colours, showing shorter lifetime components in certain chromosomes at heterochromatin region (red regions) compared to other chromosomes, lifetime change was also observed at interphase, in a nucleus (A). Chromosomes number is 46 in both A and B images, scale bar-5µm (A) and 10µm (B). Colour scale shows lifetime variation in A, B and C; red represents shorter lifetime and blue longer lifetime change. Dashed arrow shows extra damaged chromosomes (21) with lifetime changes (A and B). And, C) close-up image of chromosome 21.

Chromosome A	Mean lifetime ± SD, (ns)
1	2.98 ± 0.02
9	2.94 ± 0.00
15	2.96 ± 0.01
16	2.95 ± 0.00
Y	2.98
21	2.98 ± 0.02

.

Table 1: A) Lifetime value of DAPI stained, of each heterochromatic region calculated from two metaphase spreads at 0.1Gy dose (fig 13). Red coloured row represents one extra chromosome appeared with lifetime change in both the spreads (fig 13 A and B).

Lifetime values were found to increase in X-ray irradiated metaphase spreads compared with non-irradiated chromosome spreads. This suggests that chromosomes lose their compaction in X-ray induced cells. We observe significant lifetime change, to 2.9ns, at telomere region in one of the chromosomes, labelled as chromosome 21 in the 0.1Gy (fig 13) X-ray induced cell.

4.3.2 Aberrations after 24hrs of irradiation at 0.2Gy

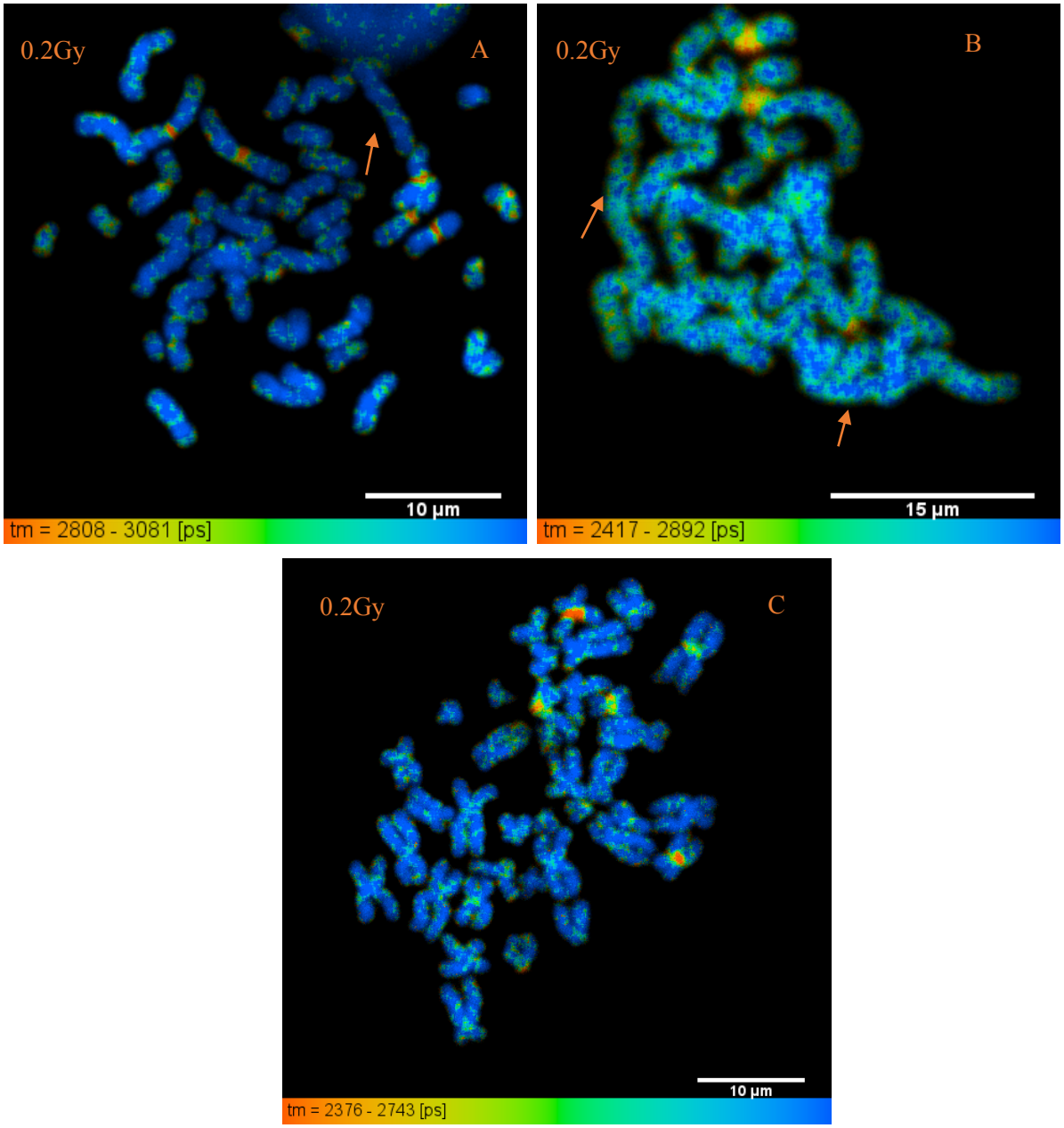

Figure 14: FLIM image of irradiated fixed human metaphase chromosomes stained with 4µM DAPI and imaged with 60x water objective. Three different spreads of metaphase chromosomes extracted after 24hrs of irradiation at 0.2Gy dose. Pseudo colours, showing shorter lifetime components in certain chromosomes at heterochromatin regions (red colour) compared to whole chromosomes. Metaphase chromosome spreads A) 43-chromosomes, scale bar-10µm B) 25-chromosomes, scale bar-15µm and C) 37-chromosomes scale bar-10µm) and colour scale shows lifetime variation in A, B and C. Arrow shows the presence of number of dicentric chromosomes in each spread.

A Chromosome	Mean lifetime ± SD, (ns)
1	2.80 ± 0.00
9	2.89
15	2.92 ± 0.07
16	2.86 ± 0.03

B Chromosome	Mean lifetime ± SD, (ns)
1	2.59
9	2.58
15	2.54 ± 0.00

C Chromosome	Mean lifetime ± SD, (ns)
1	2.61
9	2.39
15	2.42 ± 0.01
16	2.51 ± 0.05

D Chromosome	Mean lifetime ± SD, (ns)
1	2.67 ± 0.10
9	2.62 ± 0.21
15	2.63 ± 0.21

Table 2: Calculated mean lifetimes value of DAPI stained of each heterochromatic region from spread A, B and C (Fig 14). D) Averaged and pooled mean lifetime of chromosomes 1,9 and 15 from each spread of fig 14. Standard Deviation (SD) represents varied lifetime at heterochromatic regions of each autosomes.

4.3.3 Aberrations after 48hrs of irradiation at 0.2Gy

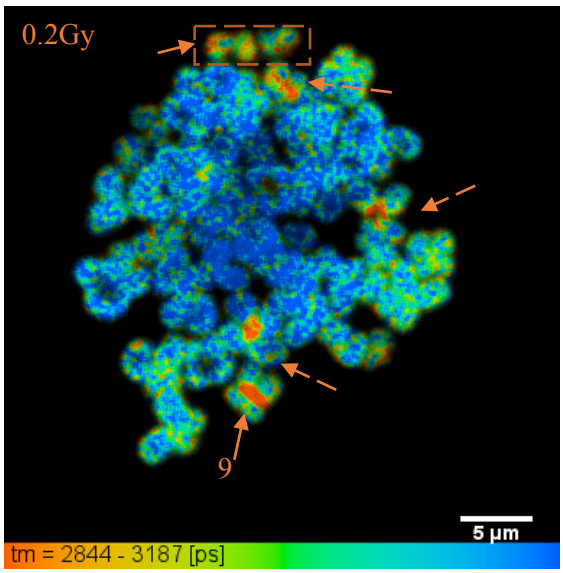

Figure 15: FLIM image of irradiated fixed human metaphase chromosomes stained with 4µM DAPI and imaged with 60x water objective. The metaphase spread after 48hrs of irradiation at 0.2Gy dose. Pseudo red colour represents the shorter lifetime components in certain chromosomes. The dashed box shows two fragmented chromosomes. The colour scale shows lifetime variations from short to long, scale bar-5µm.

Chromosome	Mean lifetime (ns)
9	2.94
Fragment-1	2.94
Fragment-2	2.97
Unknown	3.00
Unknown	2.97
Unknown	3.01

Table 3: Lifetime value of DAPI stained of each heterochromatic region calculated from one (0.2Gy dose) metaphase spread extracted after 48hrs of radiation (fig 15).

4.3.4 Aberrations after 48hrs of irradiation at 0.5Gy

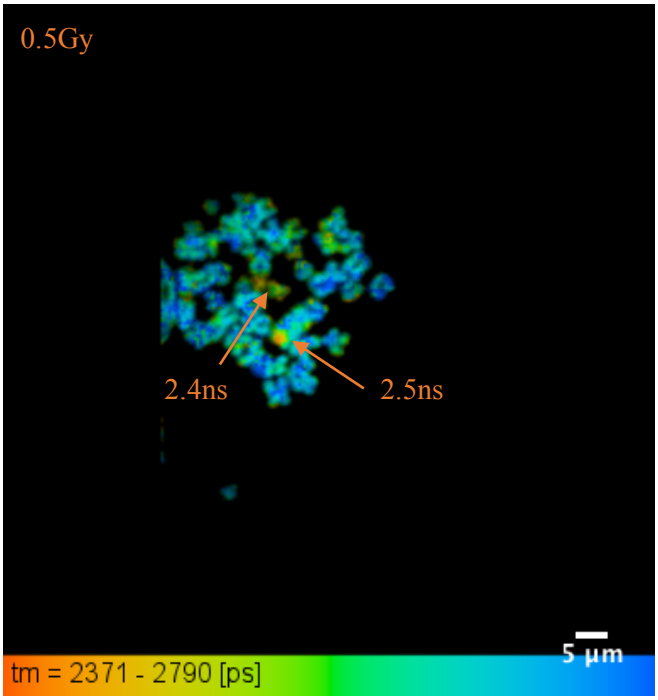

Figure 16: FLIM image of irradiated fixed human metaphase chromosomes stained with 4µM DAPI and imaged with 60x water objective. The metaphase spread after 48hrs of irradiation at 0.5Gy dose. Pseudo red colour represents shorter lifetime components in certain chromosomes, dashed box shows two fragmented chromosomes. The colour scale shows lifetime variations from short to long, scale bar-5µm.

Fig 16 shows that chromosomes loses its compact heterochromatic regions present out of nine non-X-ray irradiated chromosomes. just two of the chromosomes are showing low lifetime (red pseudo colour region present on the chromosomes) compared to other chromosomes present in the spread (fig 16).

5. DISCUSSION AND CONCLUSIONS

The main objective of this project is to understand the effects of radiation on the compaction of the chromosomes and other structural damage caused to the chromosomes in X-ray induced cells. These investigations are being done using the FLIM technique, which is sensitive to the molecular environment. The combined techniques of laser scanning confocal microscopy and multiphoton microscopy are being used to study the compaction and the condensation rate of chromatin during mitotic cell division [5,6]. According to *Estandarte et al*, 2016, lifetime changes in DAPI stained metaphase chromosomes show the presence of condensed and de-condensed regions along the length of the chromosomes, measured by FLIM.

In principle, FLIM can measure the rate of compaction in metaphase spreads, through its sensitivity to the molecular environment due to pH change, viscosity, ion concentration [4] etc. With this strong correlation of DAPI lifetime change and its sensitivity, we investigated X-ray induced cell at 250KVp energy. Irradiation is known to cause several significant structural [44] and numerical [45] chromosomal aberrations depending upon the dose and maybe the dose rate (in live cells). The DNA double strand breaks, gene sequence rearrangements and recombination are the major aberrations at the initial stage, which continues to chromosomal aberrations in future cell generations [25]. The aberrations range from point mutations to a missing set of homologous chromosomes, which further leads to lethal and non-lethal diseases including cancer.

5.1 Observed chromosome aberrations in the spreads

In our experiments, the chromosome extraction process was optimised after several trials. The aim was to get all 46 metaphase human chromosomes from the same nucleus, clustered together in a "spread", all within one image frame. An aliquot of metaphase chromosomes was dropped onto the glass slides and imaged using the fluorescence microscope to choose good spreads and to locate number of aberrations in each spread at different doses. However, troubleshooting the location of 46 metaphase chromosomes on the slide during imaging was an extremely difficult and time-consuming process. After a long struggle, a few metaphase chromosomes spreads were observed. We found certain number of dicentrics (fig 9 and 10), ring chromosome (fig 11) after 26hrs, 48hrs and 50hrs of irradiation respectively. Moreover, we also saw fused, smashed chromosomes arms (fig 8), fragmented chromosomes (fig 11)-

scaled to 0.5µm. Furthermore, these samples were taken to perform a FLIM analysis to identify the chromosomes known to contain heterochromatic regions, as reported in the literature (fig 17 A).

A

Chromosome #	Mean Lifetime ± SD, ns
1	2.58 ± 0.06
9a	2.38 ± 0.06
9b	2.21 ± 0.05
15	2.43 ± 0.05
16	2.55 ± 0.06
Y	2.58 ± 0.03

B

Chromosomes	Mean lifetime ± SD, (ns)
1	2.71 ±0.06
9	2.63 ±0.06
15	2.60 ±0.11
16	2.60 ±0.10
Y	2.55 ±0.09

Figure 17: Lifetime value of DAPI stained of each metaphase heterochromatic regions, averaged and pooled. A) from 12 non-X-irradiated chromosome spreads [5], B) from 5 non-X-ray-irradiated chromosomes spreads. SD represents varied lifetime in a heterochromatic region of a chromosome.

After further analyses, it was observed that heterochromatic chromosomes showed changes in lifetime beyond the values reported in the literature (fig 17 A). It was observed that even the repeat experiments showed lifetime change in all nine heterochromatin regions (fig 17 B) of metaphase chromosomes. However, the lifetime changes were a bit higher (ranges from 0.03ns to 0.25ns) than the values in the literature [5]. This could be due to the sample preparation methods or analysis error, but it does prove that literature [5] results are reproducible.

Nevertheless, these repeated experimental results from non-X-ray irradiated chromosomes encouraged us to apply the same technique to the X-ray irradiated chromosomes. We expects that FLIM can identify chromosomal structural aberrations in an X-ray induced cells, which are not picked up by FISH/mFISH. We note that FISH/mFISH has the ability to find only inter-chromosomal aberrations (large cross changes), such as translocations [46].

5.2 Aberration in a chromosome 21

We imaged spreads under combined laser confocal microscopy and FLIM microscopy to measure lifetime changes in a damaged metaphase spreads, because it gives information about the sub-cellular activities of the process happening in the molecules. After 24hrs of irradiation with 0.1Gy, we could manage to see all nine heterochromatic chromosomes (1, 9, 15, 16 and Y) similar to undamaged chromosomes [5]. We hypothesized the presence of one extra heterochromatic chromosome, possibly chromosome 21. Though, this shows shorter lifetime at telomere region rather than at centromere position. This could be because in a chromosome 21, DNA satellites are present at the telomere region in the short arm of the chromosome which may make it more prone to radiation damage [47]. Although, even with low doses of irradiation, the telomere ends become sticky and can adhere foreign bodies which also leads to aberrations. The telomeres contain repetitive sequences that makes them more prone to irradiation damage. We plan to look in future experiments with more statistical data to test our hypothesis.

5.3 Loss of the compaction of the chromosomes

Although we see all nine heterochromatic chromosomes, the lifetime changes at the heterochromatic regions are greater for the 0.1Gy irradiated chromosomes (Table 1), with a difference ranging from 0.3ns to 0.5ns compared with the undamaged chromosomes. We suspect that X-ray irradiation at 0.1Gy has unwound or disrupted the condensed nature of the heterochromatic regions. The difference in lifetime obtained at compact regions in a damaged chromosome might predicate the onset of severe aberrations in consecutive cell division process. Furthermore, at 0.2Gy dose, the lifetime changes at heterochromatic regions become shorter compared to 0.1Gy dose and closer to undamaged chromosomes (fig 14). The difference in lifetime change compared to undamaged chromosomes ranged between 0.01ns to 0.19ns (fig 18).

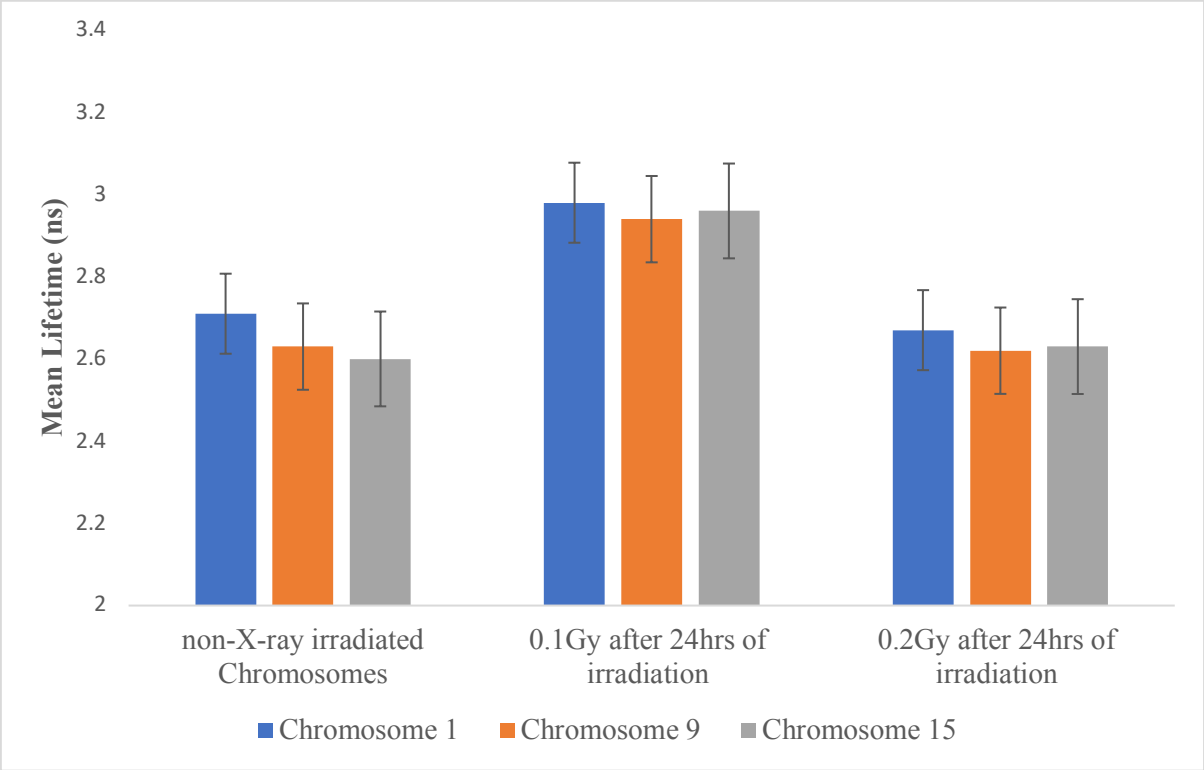

Figure 18: Lifetime changes of X-ray irradiated (0.1Gy & 0.2Gy after 24hrs of irradiation) and non-X-ray irradiated (undamaged) fixed human metaphase chromosomes 1,9 & 15. Error bars represent the deviation in a measurement.

Although, after 48 hours of irradiation at 0.2Gy, we saw some fragments of chromosomes with lifetime of 2.94ns and 2.97ns (fig 15), this shows that chromosomes might have gone through aberration such as dicentric and ring formations. It means the formation of a ring and dicentric chromosome leaves fragments of chromosomes to form other structural chromosome aberrations like ring/dicentric (fig 4). Also, we saw only few number of chromosomes showed shorter lifetime at the heterochromatic region compared to chromosomes present in the dose 0.1Gy (fig 13) and the 0.2Gy (fig 14) after 24hrs of irradiation. Particular chromosomes carried aberration will be test by mFISH method in future.

5.4 Reduced number of chromosomes from the spreads

We observed the number of missing chromosomes from the spread especially for chromosome Y, which is not been seen in all three spreads in fig 14. Moreover, one out of each paired homologous chromosomes, chromosomes 1 and 9 were found missing from the spreads. This could be because they might have lost their condensed heterochromatic region, or went through

severe structural aberrations such as micronuclei formation, also known as chromosome fragments [48] which is not picked up by FLIM.

At a 0.2Gy (fig 14) dose, the number of missing chromosomes were observed in different spreads obtained from different nucleus. This could be because it might not have been going through proper cell division process, which leads to mis-segregation of chromosomes at anaphase of the cell cycle [49]. Though, at lower dose it is not lethal to a cell but at higher dose ranging from 5Gy to 10Gy, leads to a cell death because of huge mistakes in the segregation of the chromosomes. Hence, some nuclei show incomplete number of a metaphase spreads as radiation dose increases.

Moreover, the normal cells irradiated with X-rays showed a smaller number of chromosomal aberrations compared to the cancerous cells at a low dose of irradiation. Because faster growing cells have higher chance of aberrations than normal cells even at low dose. At a low dose of X-rays, mutations can occur due to genomic instability, DNA methylation, mini and microsatellite dis-balance [50] and can carry over to the progeny. On other hand, cells can become cancerous even at 0.01Gy - 0.05Gy of an X-ray exposure [50].

Because the spread in fig 15 is clustered together, it is difficult to recognise the aberrations. Nevertheless, we still see short lifetime components in the second mitotic cell cycle. It has been reported in the literature that the number of dicentric chromosomes reduces in number at the second and the third cell division but it might have gone through other aberrations which is not clear in the spreads[49]. Though, enough metaphase spreads were not observed due to cell death at higher doses rate. Unfortunately, enough data is still not available to give statistically meaningful results.

To get clear information about the quantitative and qualitative aberrations due to ionising irradiation, FLIM and mFISH can be used together to understand the aberrations in different chromosomes carrying aberrations at different doses rates. Also, it is important to look at the transmission of chromosome aberrations in subsequent cell divisions.

5.5 Summary

This has been observed throughout our experiments so far that the chromosomes extracted from the B-lymphocytes cells were very sensitive to X-ray irradiation and they could easily get damaged even with low radiation doses. Various chromosomal aberration shown in the report such as dicentrics, smashed arms, fragments and ring chromosomes all occurred at low radiation dose. At a very high dose, such as 5Gy-10Gy, very few cells were observed and metaphase spreads were not in a complete set of 46 chromosomes. This may be because the chromosomes behave uniquely at different radiation doses which made it bit difficult to produce concrete results from each radiation dose. A actions need to be taken to improve the spreads of a metaphase chromosomes at each radiation doses. This will be improved by taking an average of 30-40 good spreads using a Metafer software available from the Metasystems, which counts metaphase chromosomes automatically, present on the slides. These spreads will be investigated by FLIM followed by mFISH to locate chromosomes carry aberrations.

6. FUTURE WORK

My Gantt chart (Fig 19) focus on my PhD plan for 2018-2019 work to be done. This includes chromosome preparations at different environmental conditions such as X-ray irradiated and heavy metal staining of chromosomes. In addition, I am also planning to prepare condensed and de-condensed chromosomes using divalent cations (Mg^{+2} and Ca^{+2}). All these prepared chromosome samples will be imaged using FLIM, X-ray ptychography and Fluorophore Localisation Imaging with Photo-bleaching (FLImP) methods.

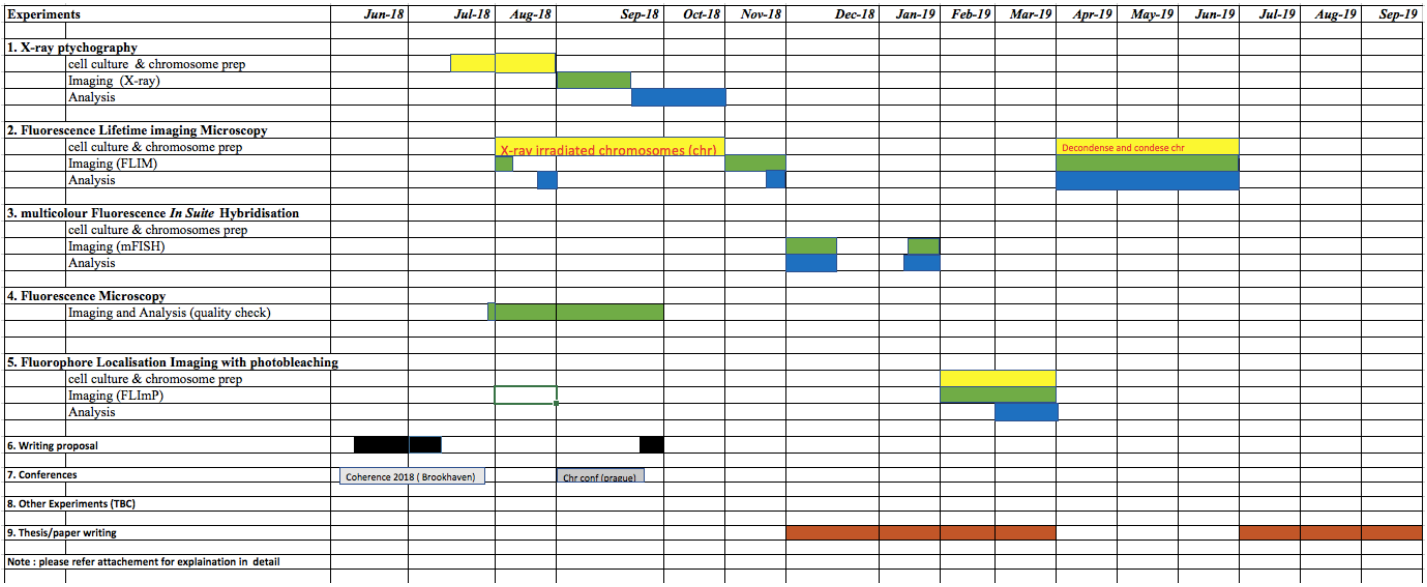

Figure 19: PhD plan for 2018-2019.

6.1 Short term goals

I have shown in my transfer report that FLIM is a technique that can be used to study the X-ray induced chromosomal aberrations. Specifically, I have seen the aberrations which affect the compaction of the chromatins like heterochromatin regions present along the length of the chromosomes. The future studies towards this project will be deeply focused on the compaction and the structural aberrations such as dicentrics, translocations and ring chromosome formations occurred due to irradiation. In future, it may be helpful to diagnose genomic instability and consequent diseases.

In this transfer report, we saw some aberrations such as dicentrics (fig 9 and 10), ring chromosomes (fig 11) and possibility of chromosomes fragments (fig 10 and 11). These

samples have been preserved and will be taken for FLIM imaging to see the lifetime change in damaged chromosomes.

My aim is to investigate, first (24hrs), second (48hrs) and third (72hrs) generations of a cell division to see the number of aberrations occurring and which have continued to the next generations. The X-ray doses chosen to study structural chromosomes aberrations are 0.1Gy, 0.2Gy, 0.5Gy 1Gy, 2Gy and 5Gy. The metaphase chromosomes will be extracted from the irradiated cells, fixed with the methanol acetic acid and stained with a DAPI for imaging. It has been reported in the literature that the dicentric aberrations starts decreasing with the increasing numbers of mitotic cell division although number of ring chromosomes increase [27]. Therefore, this study might help us to discover the proportion ratio of a dicentrics and the ring chromosomes with the consequent cell division in an X-ray induced cells. An average of 30-40 different metaphase spreads will be needed for statistical data at each radiation dose. Including all the consequent mitotic cell divisions, a large amount of data will be needed for significant results.

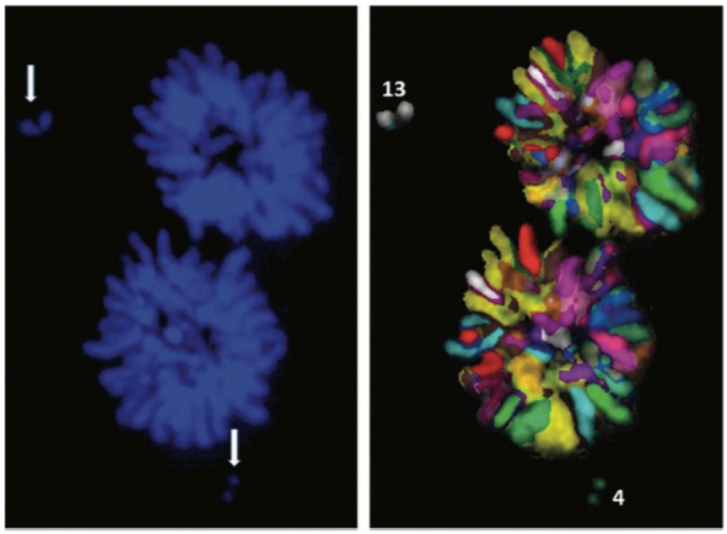

Figure 20: The detection of chromosome fragments originated from chromosome 4 and 13 (arrow) at anaphase of the cell cycle in a γ-rays irradiated peripheral blood lymphocyte at dose of a 2Gy using mFISH [48].

However, FLIM is rather slow for characterization of the individual chromosomes to look for aberrations. I will therefore employ multicolour FISH to label the whole genome and produce a karyotype. The combination of FLIM and mFISH will be helpful to locate the chromosomes which contain aberrations and understand the condensation state. However, it will give a better approach to understand the events following due to irradiation damage. Accordingly, after

measurement of a lifetime using FLIM it would be interesting to see particular chromosomes containing specific aberrations and the number of aberrations occurred in each mitotic chromosome using mFISH. We saw some aberrations such as dicentrics (fig 14) and the possibility of chromosome fragments (fig 15) but it is not clear which individual chromosome contain aberrations. Therefore, the mFISH can be potentially helpful technique to identify chromosomes containing aberrations. As its shown in fig 20, that mFISH as the ability to detect even the fragments originated from a aberrated chromosome.

6.1.1 mFISH on 0.1Gy dose after 24hrs of irradiation

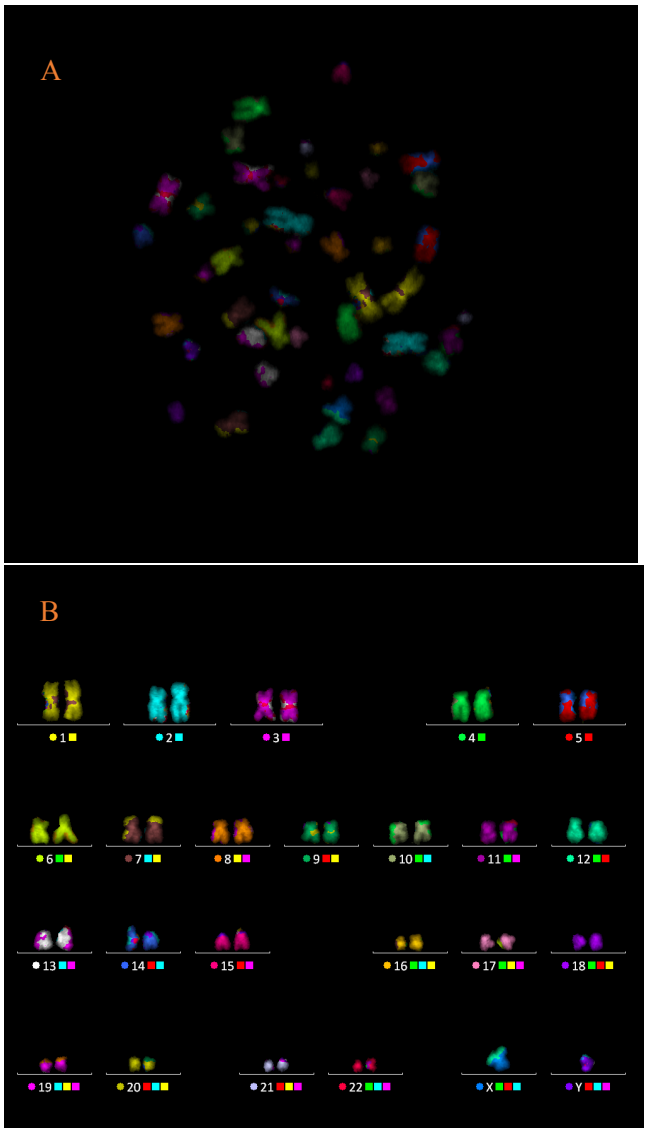

Figure 21: Detection of chromosomal aberration obtained from a 0.1Gy dose after 24hrs of irradiation, using mFISH. A) Spread from a nuclei B) Karyotype of a fig 21, A.

The preliminary result from mFISH data shows that there are few translocation aberrations took place between chromosomes i) chromosome 1 and 7, ii) chromosome 4 and 10, and iii) chromosomes 5 and 14. As mFISH has the ability to pick up the major aberrations such as translocations and the fragments obtained from a chromosome [44,48]. Therefore, mFISH being use along with FLIM to investigate chromosomes aberrations caused due to X-ray irradiations.

6.2 Experimental plans

1) **X-ray Ptychography on a human chromosomes (Beamtime in September 2018).**
   a) Prepare chromosome spreads from:
      i) X-ray radiated metaphase chromosomes (consider doses: 0.1Gy, 0.2Gy and 0.5Gy).
      ii) Decondensed and condensed chromosomes (by using different concentrations of Magnesium chloride and Calcium chloride).
      iii) Also prepare unstained and stained samples (stains using such as Platinum and Uranyl acetate).

      Note : All samples are mounted on TEM grids and taken to X-ray imaging.

   b) Reconstruct data by ptychography and produce karyotype from reconstructed image.

   Outcome : Will help us to karyotype various chromosome samples prepared in a different environment conditions to see the total DNA content in each spread.

2) **Investigation of human chromosome compaction by FLIM (Fluorescence Lifetime Imaging Microscopy) (Proposing beamtime).**
   a) Prepare chromosome spreads from:
      i) X-ray radiated metaphase chromosomes (consider doses: 0.1Gy, 0.2Gy and 0.5Gy).
      ii) Decondensed and condensed chromosomes (by using different concentrations of Magnesium chloride and Calcium chloride).

      Note : All samples are mounted on glass slides/coverslips and taken to FLIM imaging.

   b) FLIM will also be done on different generations of cell division after radiation dose (Consider generations: 24hrs, 48hrs and 72hrs after irradiation).
   c) Obtained data will be analysed using SPCImage software.

   Outcome : Will help us to find gain or loss of a compaction in the chromosomes.

3) **Investigation of major chromosomal aberrations using mFISH (multicolour-Fluorescence In Suite Hybridisation).**
   a) Prepare chromosome spreads from:

i) X-ray radiated metaphase chromosomes (consider doses: 0.1Gy, 0.2Gy and 0.5Gy).

Note : All samples are mounted on glass slides/coverslips, these samples will first be imaged with FLIM and then mFISH.

b) Data will be analysed using ISIS software available from MetaSystem.

Outcome : Will help us to karyotype irradiated and non-irradiated chromosomes

4) Investigation of human chromosomes using Fluorescence Microscopy.

a) Prepare chromosome spreads from:

i) X-ray radiated metaphase chromosomes (consider doses: 0.1Gy, 0.2Gy and 0.5Gy).

ii) Decondensed and condensed chromosomes (by using different concentrations of Magnesium chloride and Calcium chloride).

iii) Also prepare unstained and stained samples (stains using such as Platinum and Uranyl acetate)

Note : All samples are mounted on glass slides and stained with DAPI dye for analysis.

Outcome : i) To analyse the quality and to locate the chromosome samples for the actual experiments.

ii) To investigate a numerical chromosomal aberrations due to ionising radiation.

5) To study the structure of human chromosome using FLImP (Fluorophore Localisation Imaging with Photobleaching) (proposing beamtime).

a) Prepare metaphase human chromosome spreads and stained with YOYO dye (staining method still needs to be optimised).

Note : All samples will be prepared in 3mm petri dish.

Outcome: To resolve the question of the existence of the controversial 30nm chromatin fibre within human chromosomes.

7. REFERENCES

1 D. L. Preston, *Disaster Med Public Heal. Prep.*, 2014, **5**, 1–24.
2 L. S. Cram, M. F. Bartholdi, F. A. Ray, J. Meyne, R. K. Moyzis, T. Schwarzacher-Robinson and P. M. Kraemer, *Cytometry*, 1988, **9**, 94–100.
3 W. Becker, *J. Microsc.*, 2012, **247**, 119–136.
4 K. Suhling, L. M. Hirvonen, J. A. Levitt, P.-H. Chung, C. Tregidgo, A. Le Marois, D. A. Rusakov, K. Zheng, S. Ameer-Beg, S. Poland, S. Coelho, R. Henderson and N. Krstajic, *Med. Photonics*, 2015, **27**, 3–40.
5 A. K. Estandarte, S. Botchway, C. Lynch, M. Yusuf and I. Robinson, *Sci. Rep.*, 2016, **6**, 31417.
6 R. Phengchat, H. Takata, K. Morii, N. Inada, H. Murakoshi, S. Uchiyama and K. Fukui, *Sci. Rep.*, 2016, **6**, 38281.
7 A. Travers, *Sci. (New York, NY)*, 2014, **344**, 370–372.
8 K. Maeshima and M. Eltsov, *J. Biochem.*, 2008, **143**, 145–153.
9 D. J. Tremethick, *Cell*, 2007, **128**, 651–654.
10 K. Maeshima, R. Imai, S. Tamura and T. Nozaki, *Chromosoma*, 2014, **123**, 225–237.
11 W. J. Wall, in *The Search for Human Chromosomes*, Springer International Publishing, Switzerland, 1st edn., 2016, pp. 85–102.
12 A. T. Sumner, *Cancer Genet. Cytogenet.*, 1982, **6**, 59–87.
13 J. C. Hozier, L. T. Furcht and G. Wendelshafer-grabb, *Chromosoma*, 1981, **64**, 55–64.
14 H. Huang and J. Chen, in *Cancer Cytogenetics*, ed. T. (eds) Wan, Humana Press, New York, 2017, pp. 59–66.
15 A. K. Jain, D. Singh, K. Dubey, R. Maurya and A. K. Pandey, in *Mutagenicity:Assays and Applications*, eds. A. Kumar, V. Dobrovolsky, A. Dhawan and R. Shanker, Academic Press, Ahemdabad, India, 1st edn., 2017, pp. 69–83.
16 M. E. Lomax, L. K. Folkes and P. O. Neill, *Clin. Oncol.*, 2013, **25**, 578–585.
17 O. Desouky, N. Ding and G. Zhou, *J. Radiat. Res. Appl. Sci.*, 2015, **8**, 247–254.
18 D. Azzam, E. Jay-Gerin, J. Pain, *Cancer Lett.*, 2014, **327**, 48–60.
19 S. F. AbdulSalam, F. S. Thowfeik and E. J. Merino, *Biochemistry*, 2017, **55**, 5341–5352.
20 B. Schwer, P. Wei, A. N. Chang and J. Kao, *Proc. Natl. Acad. Sci. U. S. A.*, 2016, **113**, 2258–2263.
21 M. Ojima, M. Ito, K. Suzuki and M. Kai, *PLoS One*, 2015, 1–13.
22 C. Blanpain, M. Mohrin, P. A. Sotiropoulou and E. Passegue, *Cell Stem Cell*, 2011, **8**, 16–29.
23 E. Tobias, in *Essential Medical Genetics*, Wiley-Blackwell, Singapore, 6th edn., 2011, pp. 89–111.
24 N. B. Ouchi, in *Evolution of Ionizing Radiation Research*, ed. M. Nenoi, IntechOpen, 2015, pp. 41–62.
25 T. Aparicio, R. Baer and J. Gautier, *DNA Repair*, 2015, **19**, 169–175.
26 M. Borràs-fresneda, J. Barquinero, M. Gomolka and S. Hornhardt, *Sci. Rep.*, 2016, **6:27043**, 1–11.
27 T. H. Ryu, J. H. Kim and J. K. Kim, *Genome Integr.*, 2016, **7: 5**, 3–5.
28 A. Kaddour, B. Colicchio, D. Buron, E. El Maalouf, E. Laplagne, M. Ricoul, A. Lenain, W. M. Hempel, L. Morat, M. Al Jawhari, C. Cuceu, L. Heidingsfelder, E. Jeandidier, G. Deschênes, M. El May, T. Girinsky and A. Bennaceur-griscelli, *Sci.*

Rep., 2017, **7: 3291**, 1–11.
29 R. Bishop, *Biosci. Horizons*, 2010, **3**, 85–95.
30 R. Anderson, in *Fluorescence in situ Hybridization (FISH) Protocols and Applications*, eds. J. M. Bridger and E. V Volpi, Humana Press, Totowa NJ, 2010, pp. 83–97.
31 K. Tsukada, G. Imataka and H. Suzumura, *Cell Biochem Biophys*, 2012, **63**, 191–198.
32 P. A. Muehlbauer and M. J. Schuler, *Mutat. Res.*, 2005, **585**, 156–169.
33 S. T. Spagnol and K. N. Dahl, *PLoS One*, 2016, **11**, 1–19.
34 G. Yahav, A. Hirshberg, O. Salomon, N. Amariglio, L. Trakhtenbrot and D. Fixler, *Cytom. Part A*, 2016, **89A**, 644–652.
35 J. R. Lakowicz, in *Principles of Fluorescence Spectroscopy*, Springer, Boston, MA, 3rd edn., 2006, pp. 1–26.
36 C. Wang and C. Bai, in *Single Molecule Chemistry and Physics-An Introduction*, Springer-Verlag Berlin Heidelberg, Beijing, China, 1st edn., 2006, pp. 183–190.
37 J. R. Lakowicz, in *Principles of Fluorescence Spectroscopy*, Springer, Boston, MA, 3rd edn., 2006, pp. 741–755.
38 S. Laptenok, K. M. Mullen, J. W. Borst, I. H. M. va. Stokkum, V. V Apanasovich and A. J. W. . Visser, *J. Stat. Softw.*, 2007, **18**, 1–20.
39 M. L. Barcellona and E. Gratton, *Eur. Biophys. J.*, 1990, **17**, 315–323.
40 T. F. Scientific, in *The Molecular probes handbook*, ThermoFisher Scientific, United States, 11th edn.
41 C. L. Kielkopf, S. White, J. W. Szewczyk, J. M. Turner, E. E. Baird, P. B. Dervan and D. C. Rees, *Proc. Natl. Acad. Sci. U. S. A.*, 1998, **282**, 111–115.
42 R. Won, K. Leung, S. A. Yeh and Q. Fang, 2011, **2**, 2517–2531.
43 M. Y. Berezin and S. Achilefu, *Chem. Rev.*, 2011, **110**, 2641–2684.
44 R. M. Anderson, N. D. Sumption, D. G. Papworth and D. T. Goodhead, *Int. J. Radiat. Biol.*, 2006, **82**, 49–58.
45 Y. Cho, S. Kim, H. Woo, Y. Kim, S. Ha and H. Chung, *Int. J. Environ. Res. Public Health*, 2015, **12**, 15162–15172.
46 R. M. Anderson, D. L. Stevens and D. T. Goodhead, *Proc. Natl. Acad. Sci. U. S. A.*, 2002, **99**, 12167–12172.
47 T. C. Hsu, in *Human and Mammalian Cytogenetics: An Historical Perspective*, Springer, New York, 1979, pp. 60–70.
48 A. S. Balajee, A. Bertucci, M. Taveras and D. J. Brenner, *Mutagenesis*, 2014, **29**, 447–455.
49 A. Janssen, G. J. P. L. Kops and R. H. Medema, *Proc. Natl. Acad. Sci. U. S. A.*, 2009, **106**, 19108–19113.
50 M. S. Linet, T. L. Slovis, D. L. Miller, R. Kleinerman, C. Lee, P. Rajaraman and A. B. De Gonzalez, *CA. Cancer J. Clin.*, 2012, **62**, 75–100.